Chinese Journal of Aeronautics, (2016), 29(4): 962–971

Chinese Society of Aeronautics and Astronautics
& Beihang University

Chinese Journal of Aeronautics

cja@buaa.edu.cn
www.sciencedirect.com

Advanced multiple response surface method of sensitivity analysis for turbine blisk reliability with multi-physics coupling

Zhang Chunyi [a], **Song Lukai** [a,b], **Fei Chengwei** [b,c,*], **Lu Cheng** [a], **Xie Yongmei** [a]

[a] *School of Mechanical and Power Engineering, Harbin University of Science and Technology, Harbin 150080, China*
[b] *School of Energy and Power Engineering, Beihang University, Beijing 100083, China*
[c] *Department of Mechanical Engineering, The Hong Kong Polytechnic University, Kowloon 999077, China*

Received 24 June 2015; revised 31 May 2016; accepted 2 June 2016
Available online 27 June 2016

KEYWORDS

Advanced multiple response surface method;
Artificial neural network;
Intelligent algorithm;
Multi-failure mode;
Reliability analysis;
Turbine blisk

Abstract To reasonably implement the reliability analysis and describe the significance of influencing parameters for the multi-failure modes of turbine blisk, advanced multiple response surface method (AMRSM) was proposed for multi-failure mode sensitivity analysis for reliability. The mathematical model of AMRSM was established and the basic principle of multi-failure mode sensitivity analysis for reliability with AMRSM was given. The important parameters of turbine blisk failures are obtained by the multi-failure mode sensitivity analysis of turbine blisk. Through the reliability sensitivity analyses of multiple failure modes (deformation, stress and strain) with the proposed method considering fluid–thermal–solid interaction, it is shown that the comprehensive reliability of turbine blisk is 0.9931 when the allowable deformation, stress and strain are 3.7×10^{-3} m, 1.0023×10^{9} Pa and 1.05×10^{-2} m/m, respectively; the main impact factors of turbine blisk failure are gas velocity, gas temperature and rotational speed. As demonstrated in the comparison of methods (Monte Carlo (MC) method, traditional response surface method (RSM), multiple response surface method (MRSM) and AMRSM), the proposed AMRSM improves computational efficiency with acceptable computational accuracy. The efforts of this study provide the AMRSM with high precision and efficiency for multi-failure mode reliability analysis, and offer a useful insight for the reliability optimization design of multi-failure mode structure.

* Corresponding author. Tel. +852 34002600.
E-mail addresses: zhangchunyi@hrbust.edu.cn (C. Zhang), songlukai29@163.com (L. Song), feicw544@163.com (C. Fei), liuyue501790058@qq.com (C. Lu), 939406136@qq.com (Y. Xie).

Peer review under responsibility of Editorial Committee of CJA.

Production and hosting by Elsevier

http://dx.doi.org/10.1016/j.cja.2016.06.017

1. Introduction

As the heart of aircraft, aeroengine directly influences the safety and reliability of flight.[1] Turbine blisk, as one of the core components of aeroengine, effects the reliable and stable operation of aeroengine. However, turbine blisk always bears many loads from high temperature, high pressure and high rotational velocity, and holds many failure modes in operating process, such as strain failure, deformation failure, and so forth.[2] Therefore, it is significant to carry out reasonable and effective reliability analysis.

Plentiful studies on structure reliability analysis lead to the development of reliability analysis methods.[3] For instance, Kaymaz[4] studied the structural reliability problem based on Kriging model; Lin et al.[5] discussed the reliability of coupled oscillators; Dimitrov et al.[6] proposed the model factor rectification method for the reliability analysis of composite turbine blade based on finite element technology. Hu et al.[7] completed the reliability analysis of turbine blade by the stochastic chaos polynomial expansion method approximating to structural limit-state function considering fluid dynamics. In order to solve the multi-source uncertainty problem of structure reliability analysis, Wang et al.[8] discussed the hybrid reliability analysis method based on the convex model theory and compared with the conventional probabilistic analysis method.

As an important approach, response surface method (RSM) is widely used in structural reliability analysis.[9–11] Zhang and Bai GC[9] developed extremum response surface method for the reliability analysis of two-link flexible robot manipulator; Krishnamurthy[10] compared the response surface construction methods for derivative estimation using moving least squares, Kriging and radial basis functions; Xiong et al.[11] advanced a double weighted stochastic response surface method for reliability analysis. To further improve the computational efficiency and precision, many works have been done. Fei and Bai GC[12,13] adopted support vector machine response surface method for structural reliability analysis. Ren and Bai GC[14] established artificial neural network (ANN) response surface model by integrating ANN algorithm with high accuracy and nonlinear mapping ability; Lv et al.[15] proposed the weight line response surface method based ANN for reliability analysis. To analyze the effect of high temperature heat translation on the reliability analysis of blisk structure, Bai B and Bai GC[16] completed the sensitivity analysis for blisk reliability by proposing extremum response surface method.

However, those methods are only fitted for structure reliability analysis with single failure mode. Few efforts on the multi-discipline and multi-object reliability analysis are done besides Fei et al.[17–19] Fei and Bai GC[17] proposed distributed collaborative extremum response surface method for the transient design of mechanical dynamic assembly reliability; Bai GC and Fei[18] proposed distributed collaborative response surface method for the design of mechanical dynamic assembly reliability; Zhai et al.[19] completed sensitivity analysis for the reliability of high pressure turbine blade-tip radical running clearance by adopting multiple response surface method. However, those achievements are only considered with one failure mode rather than multiple failure modes for the reliability analysis of complex structure.

The objective of this paper is to propose an advanced multiple response surface method (AMRSM) based on intelligent algorithm with high nonlinear mapping ability and response surface method for structural reliability analysis. The AMRSM mathematical model is established by integrating particle swarm optimization (PSO), ANN and multiple response surface theory. The reliability analysis of an aeroengine turbine blisk is implemented by reasonably selecting random variables and taking the deformation, stress and strain of turbine blisk as output response. Through the comparison of methods (Monte Carlo (MC) method, traditional response surface method (RSM), multiple response surface method (MRSM) and AMRSM),[19] the effectiveness and reasonability of the presented AMRSM are validated.

In what follows, in Section 2, AMRSM is studied including the basic idea and mathematical model of AMRSM and intelligent operator. Section 3 focuses on reliability sensitivity approach. The sensitivity analysis for turbine blisk reliability is achieved in Section 4. Section 5 summarizes the conclusions of this study.

2. AMRSM

2.1. MRSM

The basic thought of MRSM is shown as follows:

(1) The single response surface model between input random variables x_i and output response $y(x_i)$ is established for each failure mode of structure.
(2) Multiple response surface models are established based on single response surface model for structure reliability analysis rather than finite element method (FEM).

In line with the basic thought of MRSM, the stochastic problem of nonlinear complex structure reliability analysis is transformed into the problem of solving mathematical model, which greatly reduces computational time and improves computational efficiency.[19] The mathematical model of MERM is shown as:

$$y^{(p)} = a^{(p)} + \sum_{i=1}^{n} b_i^{(p)} x_i^{(p)} + \sum_{i=1}^{n} c_i^{(p)} \left(x_i^{(p)}\right)^2 \tag{1}$$

where $y^{(p)}$ is the pth output response; $x_i^{(p)}$ the ith component of the variable $\boldsymbol{x}$ corresponding to the pth output response; $a^{(p)}$ the constant item; $b_i^{(p)}$ the coefficients of linear polynomial; $c_i^{(p)}$ the coefficients of quadratic polynomial; n is the number of variables in $\boldsymbol{x}$.

2.2. AMRSM of structure reliability analysis

2.2.1. Basic thought of AMRSM

Reliability analysis is to adopt the random dispersion of random variables to analyze the probability that the structure meet the specified function in the practical engineering. In order to realize the comprehensive reliability analysis of multi-failure mode structure by using traditional RSM, AMRSM was advanced for structure reliability analysis on the foundation of MRSM. The basic thought is that (1) the random input variables are determined and the finite element (FE) model of structure is established; (2) according to the FE model, a number of samples are extracted as training sam-

ples; (3) the number of nodes in each layer of neural network is defined, and many neural network models are fitted to these training samples; (4) the initial optimal weights and threshold of each neural network model are searched by using PSO; (5) the multiple response surface models with neural network are built by Bayesian regularization algorithm (BRA). The output response values are obtained by MC method linkage sampling of advanced multiple response surface models. The reliability analysis procedure of turbine blisk with AMRSM is shown in Fig. 1.

2.2.2. Mathematical model of AMRSM

Arbitrary shape and strong adaptivity are the features of neural network, which may accurately fit the complex function relationship between random variables and response variable. back-propagation artificial neural network (BP-ANN) topology model is shown in Fig. 2. The function relationship between response y and input variables $\boldsymbol{x}$ can be structured as

$$y = f_2\left(\sum_{i=1}^{n} \boldsymbol{W}_{ik} f_1\left(\sum_{k=1}^{m} \boldsymbol{W}_{kj} x_i + \boldsymbol{b}_k\right) + \boldsymbol{b}_j\right) \tag{2}$$

where $\boldsymbol{W}_{ik}$ is the connection weight between the ith node of input layer and the kth node of hidden layer; $\boldsymbol{b}_k$ is the kth threshold value of hidden layer; $\boldsymbol{W}_{kj}$ is the connection weight between the kth node of hidden layer and the jth node of output layer; $\boldsymbol{b}_j$ is the jth threshold value of the output layer; $f_1(\cdot)$ and $f_2(\cdot)$ are the transfer functions of hidden layer and output

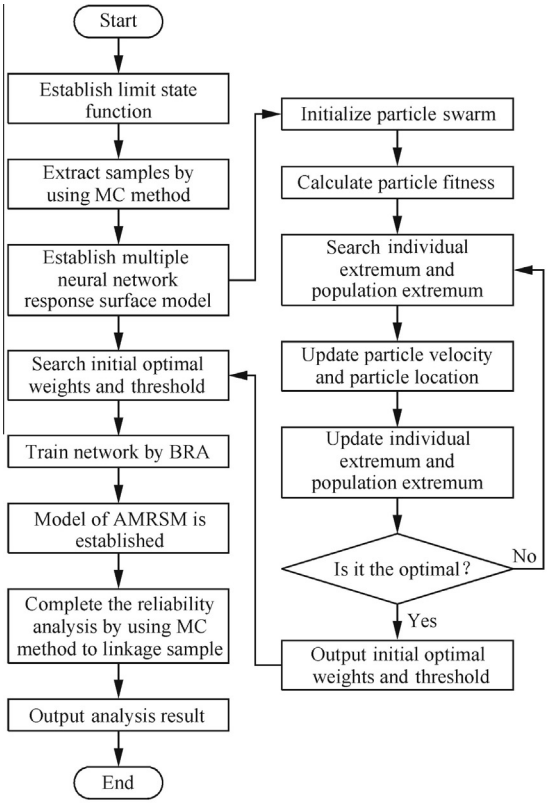

Note: MC—Monte Carlo; BRA—Bayesian regularization algorithm; AMRSM—advanced multiple response surface method.

Fig. 1 Reliability analysis procedure of turbine blisk with AMRSM.

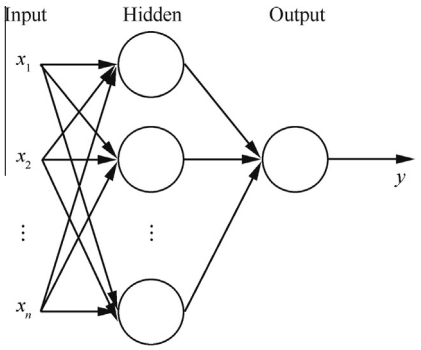

Fig. 2 Back-propagation artificial neural network (BP-ANN) topology model.

layer, respectively; m and n are the number of nodes in input layer and hidden layer, respectively.

Through the establishment of many response surface models for each failure mode, the advanced multi-response surface model is shaped as

$$\begin{cases} y^{(1)} = f_2^{(1)}\left(\sum_{i=1}^{n} W_{ik}^{(1)} f_1^{(1)}\left(\sum_{k=1}^{m} \boldsymbol{W}_{kj}^{(1)} x_i^{(1)} + b_k^{(1)}\right) + b_j^{(1)}\right) \\ y^{(2)} = f_2^{(2)}\left(\sum_{i=1}^{n} \boldsymbol{W}_{ik}^{(2)} f_1^{(2)}\left(\sum_{k=1}^{m} \boldsymbol{W}_{kj}^{(2)} x_i^{(2)} + b_k^{(2)}\right) + b_j^{(2)}\right) \\ \vdots \\ y^{(p)} = f_2^{(p)}\left(\sum_{i=1}^{n} W_{ik}^{(p)} f_1^{(p)}\left(\sum_{k=1}^{m} W_{kj}^{(p)} x_i^{(p)} + b_k^{(p)}\right) + b_j^{(p)}\right) \end{cases} \tag{3}$$

2.2.3. Intelligent operators

As a kind of emerging algorithm, intelligent algorithm is now widely employed in many fields of parallel search and pattern recognition, which is promising for addressing the complex computation problem by simulating biological evolution. Particle swarm operator is prone to premature convergence or local optimal problem during intelligent search, which seriously impacts the accuracy of network model. The training operator of general BP network has slow convergence speed, low approximation accuracy and weak generalization ability, so that the accuracy of complex structure reliability analysis is always unacceptable. Accordingly, it is significant for the improvement of the precision of reliability analysis to effectively design particle swarm operator and training operator.

Currently, the PSO has been widely applied to function optimization, neural network training and fuzzy system control due to easy realization and high searching efficiency.[20] Firstly, the number of particles is determined and each particle is initialized in space. Hereinto, each particle has a potential solution. All particles search for the optimal solution in the solution space by following current optimal particles and tracking individual extreme values and population extremum to update individual position to research for the optimal solution. The renewal particle position and velocity are

$$\begin{cases} X_{id}^{k+1} = X_{id}^{k} + V_{id}^{k+1} \\ V_{id}^{k+1} = wV_{id}^{k} + c_1 r_1 (P_{id}^{k} - X_{id}^{k}) + c_2 r_2 (P_{gd}^{k} - X_{id}^{k}) \end{cases} \tag{4}$$

where w is the inertia weight; d is the search space dimension; i is the ith particle; k is the current iteration number; V_{id} is the current particle velocity; P_{id} is the current individual extremum; P_{gd} is the current population extremum; c_1 and c_2 are the non-negative acceleration factors; r_1 and r_2 are the random numbers during time domain [0,1].

Inertia weight w reflects the degree of the current velocity inheriting the previous velocity. Larger inertia weight is beneficial to global search, while small inertia weight makes for local search. To better balance the global and local search ability, this paper adopts the adaptive inertia weight changing with iterations, i.e.,

$$w(t) = w_1 - (w_1 - w_2)t/T \tag{5}$$

where w_1 is the initial inertia weight; w_2 the inertia weight at the largest number of iteration; t the current iteration number; T the largest iteration number.

Gradient decent method is general BP network training algorithm, which does not have a good application in complex nonlinear function approximation due to low approximation accuracy and weak generalization ability. For the problem of the algorithm, BRA is chosen to train ANN model in this paper. The algorithm is able to effectively improve the generalization of ANN through solving the over-fitting problem by continuously reducing the weights and threshold values in training process. Its performance function is

$$\boldsymbol{E} = k_1\boldsymbol{E}_D + k_2\boldsymbol{E}_W \tag{6}$$

where

$$\begin{cases} \boldsymbol{E}_D = \dfrac{1}{2}||\varepsilon(\boldsymbol{W}^K + \boldsymbol{Z}(\boldsymbol{W}^{K+1} - \boldsymbol{W}^K))||^2 + \lambda||\boldsymbol{W}^{K+1} - \boldsymbol{W}^K||^2 \\ \boldsymbol{E}_W = \dfrac{1}{N}\sum\limits_{j=1}^{N}\boldsymbol{w}_j^2 \end{cases} \tag{7}$$

where k_1 and k_2 are the proportional coefficients; $\boldsymbol{w}_j$ is the weight of ANN; ε is the expected error function of output response; $\boldsymbol{W}$ is the vector of weight and threshold value for network layers; K is the iteration number; $\boldsymbol{Z}$ is the Jacobian matrix of ε; λ is the iteration variable.

3. Reliability sensitivity

The reliability sensitivity reflects the influence level of the variation of random variables on failure probability. By MC simulation, the failure probability is achieved as

$$\boldsymbol{P}_{\mathrm{f}} = 1 - \Phi\left(\frac{\boldsymbol{\mu}_g}{\sqrt{\boldsymbol{D}_g}}\right) \tag{8}$$

where $\boldsymbol{\mu}_g$ and $\boldsymbol{D}_g$ are the mean and variance matrixes of the limit state function, respectively; $\Phi(\cdot)$ is the standard normal distribution function.

The sensitivity of the mean matrix of random variables is represented by

$$\left(\frac{\partial \boldsymbol{P}_{\mathrm{f}}}{\partial \boldsymbol{\mu}}\right)_i = E\left(\frac{\lambda(\mu_{ij} - \mu_{i0})}{\sigma_{i0}^2}\right) \tag{9}$$

in which

$$\lambda = \begin{cases} 1 & y_i \geqslant [y] \\ 0 & y_i < [y] \end{cases} \tag{10}$$

in which $E(\cdot)$ is the function of mean values; μ_{ij} the jth datum in the ith input variable; μ_{i0} the mean value of the ith input variable; σ_{i0} the variance of the ith input variable; y_j the jth output response; $[y]$ the allowable deformation.

4. Example analysis

Gas turbine engine works in harsh environment so that the turbine blisk endures high temperature and high rotation speed. Therefore, it is difficult to get a coupled solution of the basic variables in fluid flow, heat transfer and structural response system simultaneously. In order to simplify the calculation under real working conditions, the relaxation coupling method was adopted to carry out the deterministic analysis of blisk considering fluid–thermal–structure interaction.

4.1. Fluid–thermal–structure interaction analysis of turbine blisk

Turbine blisk of aeroengine was taken as the object of study (Fig. 3) to validate the proposed methods. The deterministic

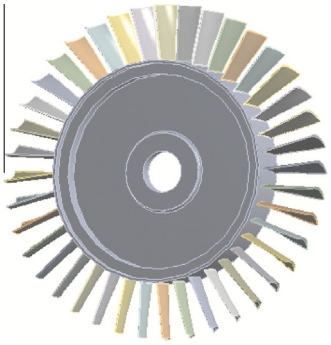

Fig. 3 Structure model of blisk.

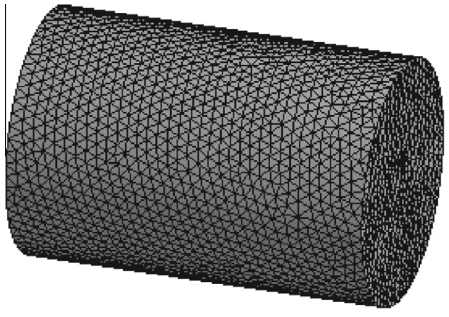

Fig. 4 Flow field grid of blisk.

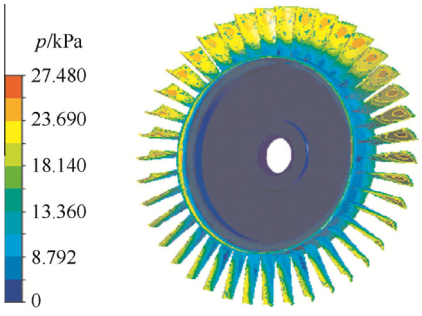

Fig. 5 Static pressure distribution of blisk surface.

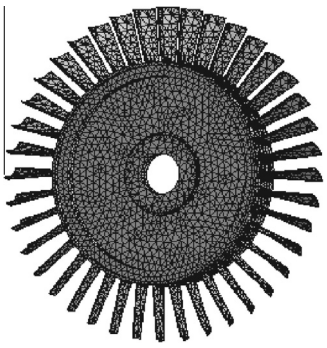

Fig. 6 Blisk grid.

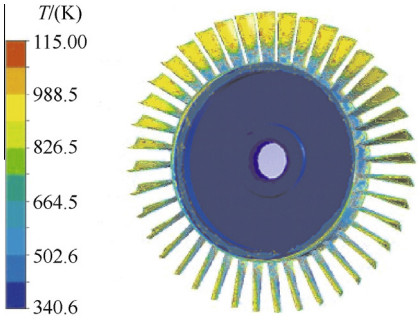

Fig. 7 Temperature distribution of blisk surface.

analysis of turbine blisk was completed under the consideration of fluid–thermal–structure interaction. The diameter of blisk is 0.75 m and the material is TC4 alloy.[21] It is assumed that inlet fluid velocity, inlet pressure, gas temperature and rotational speed are 160 m/s, 600 kPa, 1150 K and 1168 rad/s, respectively.

4.1.1. Fluid analysis of blisk

In fluid analysis, the cylinder region with the length 1.2 m and the diameter 2 m was established for the fluid field of blisk model. The fluid field zone was meshed in Fig. 4, in which the element number is 598428, and the node number is 842703. The simulation analysis of turbine blisk fluid field was executed by finite element volume method and standard k–ε turbulence model.[22] The static pressure distribution of blisk surface is shown in Fig. 5.

4.1.2. Thermal analysis on blisk

High temperature gas flow from combustion chamber imposes on the surface of blisk and thus makes blisk surface temperature rise by heat transfer and heat convection. The grid of blisk is shown in Fig. 6 where the number of element is 34875, and the number of node is 68678. The distribution of blisk surface temperature is shown in Fig. 7.

4.1.3. Structure analysis of blisk

In the analysis of blisk, the blisk material parameters and rotational speed were determined firstly. And then the fluid pressure and temperature load were loaded into the fluid–solid interface of blisk. Finally, the analyses of deformation, stress and strain were completed under the effect of fluid pressure, thermal stress and centrifugal force. The distributions of deformation, stress and strain are shown in Fig. 8. As illustrated in Fig. 8, the maximum deformation of blisk locates on blade-tip, while the maximum stress and strain of blisk are on the root of disk.

4.2. Sensitivity analysis for blisk reliability

In the light of the uncertainties of material parameters mentioned in the handbook[21] and working condition of blisk from

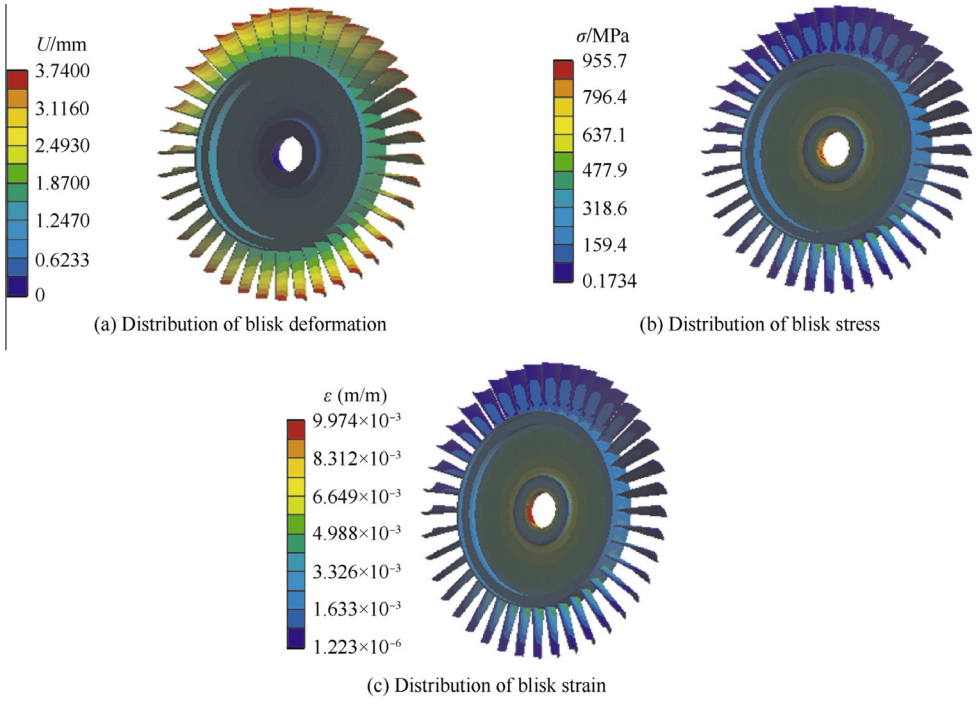

Fig. 8 Distributions of blisk deformation, stress and strain.

aeroengine tests, the inlet velocity v, inlet pressure p, temperature T, material density ρ and rotational speed ω were reasonably chosen as input random variables, which were assumed to follow normal distribution and be independent mutually. The distributions of input random variables are listed in Table 1.

The input random variables were sampled by the composite sampling technique at the location of maximum deformation, stress and strain of turbine blisk. The output response values of maximum deformation, stress and strain were obtained by the fluid–thermal–solid coupling analysis based on these samples. The normalized data were taken as the training samples of ANN. And the 5-3-1 three-layer network structure was chosen as the BP-ANN model where the transfer functions from input layer to hidden layer and hidden layer to output layer as well as the training function are 'tansig', 'purelin' and 'trainbr', respectively, and particle dimension $\theta = 16$ and particle number $N = 40$ are selected for the BP-ANN model. Through 100 iterations, the optimal fitness value curves are shown in Fig. 9.

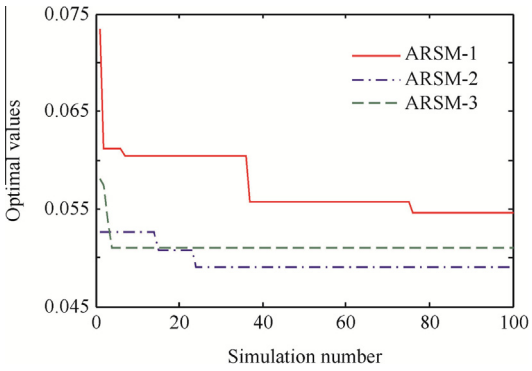

Fig. 9 Optimal fitness value curves.

As indicated in Fig. 9, the optimal fitness values are steady when the number of simulations reach at 76, 22 and 3, respectively, for deformation's ARSM (ARSM-1), stress' ARSM (ARSM-2) and strain's ARSM (ARSM-3). In other words, 76 iterations are promising to stabilize all the optimal fitness

$$\text{Deformation}\begin{cases}\boldsymbol{w}_1 = \begin{bmatrix}-0.0477 & 0.2436 & 0.0670 & -0.1283 & -0.4326\\ 0.0843 & -0.1974 & -0.1400 & -0.1369 & -0.5301\\ 0.0681 & -0.3213 & -0.2449 & 0.0713 & -0.4701\end{bmatrix}\\ \boldsymbol{b}_1 = \begin{bmatrix}-0.0071\\ 0.4961\\ -0.7749\end{bmatrix}\\ \boldsymbol{w}_2 = [-0.9486 \quad -0.8600 \quad -0.4654]\\ \boldsymbol{b}_2 = [0.0863]\end{cases} \tag{11}$$

$$\text{Stress}\begin{cases}\boldsymbol{w}_1 = \begin{bmatrix}-0.0066 & 0.0201 & -1.1554 & 0.0040 & 0.4912\\ 0.0042 & 0.0156 & 0.0134 & 0.0006 & -1.8173\\ 0.0036 & -0.0107 & -0.3930 & -0.0022 & -0.2494\end{bmatrix}\\ \boldsymbol{b}_1 = \begin{bmatrix}0.5681\\ 2.2863\\ -0.2490\end{bmatrix}\\ \boldsymbol{w}_2 = [-0.9271 \quad -1.2536 \quad -1.7726]\\ \boldsymbol{b}_2 = [1.0608]\end{cases} \tag{12}$$

$$\text{Strain}\begin{cases}\boldsymbol{w}_1 = \begin{bmatrix}0.2355 & -0.3916 & -0.2097 & -0.0784 & 0.0655\\ -0.0542 & 0.0673 & 0.1928 & -0.0055 & -1.5248\\ -0.1379 & 0.2299 & -0.4268 & 0.0508 & -0.0260\end{bmatrix}\\ \boldsymbol{b}_1 = \begin{bmatrix}-0.0107\\ 1.7311\\ -0.2104\end{bmatrix}\\ \boldsymbol{w}_2 = [-0.9541 \quad -1.0545 \quad -1.5419]\\ \boldsymbol{b}_2 = [0.4542]\end{cases} \tag{13}$$

Table 1 Distributions of input random variables.

Random variable	v (m/s)	p (kPa)	T (K)	ρ (kg/m^3)	ω (rad/s)
Mean	160	600	1150	4620	1168
Variance	3.2	18	15.56	92.4	23.36
Distribution	Gauss normal	Gauss normal	Gauss normal	Gauss normal	Gauss normal

Table 2 Results of turbine blisk reliability analysis.

Parameter	Mean	Variance	Distribution	Failure number	Reliability degree	Time (s)
Maximum deformation	3.7 mm	0.986 mm^2	Normal	55	0.9945	0.244
Maximum stress	1.0023×10^9 Pa	2.5722×10^7 Pa^2	Normal	56	0.9944	0.271
Maximum strain	0.0105 m/m	2.7883×10^{-4}	Normal	28	0.9972	0.242
Total failure mode				69	0.9931	0.761

values for three ARSMs. Therefore, the samples from 100 iterations completely satisfy the establishment of the advanced response surface model (BP-ANN model).

The initial optimal weights and threshold values are inputted into ANN model. Through network training with BRA, the advanced multiple response surface function is obtained where the weight and threshold levels of two members are shown in Eqs. (11)–(13).

Through 10000 simulations on three advanced response surfaces by MC simulation method, the output responses are obtained by inversed normalization. Based on the related parameters in an aeroengine material handbook[21] and some related material tests, it can be found that the allowable deformation, allowable stress and allowable strain are 3.7×10^{-3} m, 1.0023×10^9 Pa and 1.05×10^{-2} m/m, respectively. Referencing these material parameters, the results of turbine blisk reliability analysis are listed in Table 2. In Table 2, the failure number and the reliability are obtained by comparing the response values calculated by ARSM with the allowable values. The failure number is the number of output responses which are greater than the corresponding allowable values, while the reliability is the ratio of the number of response values, less than the corresponding allowable values, to the total response number. The curves and distributions of maximum deformation, stress and strain are shown in Figs. 10 and 11. In line with Eqs. (9) and (10), the results of sensitivity analysis for turbine blisk reliability are shown in Fig. 12 and Table 3.

4.3. AMRSM verification

To verify the AMRSM, the reliability analyses of turbine blisk were carried out with MC method, RSM, MRSM and AMRSM under the same computational conditions. All analyses are performed by the automatic parallel operation on three Intel Pentium 4 desktop computers with 2.13 GHz CPU and 4GB RAM. The computational time and reliability with four methods are shown in Tables 4 and 5.

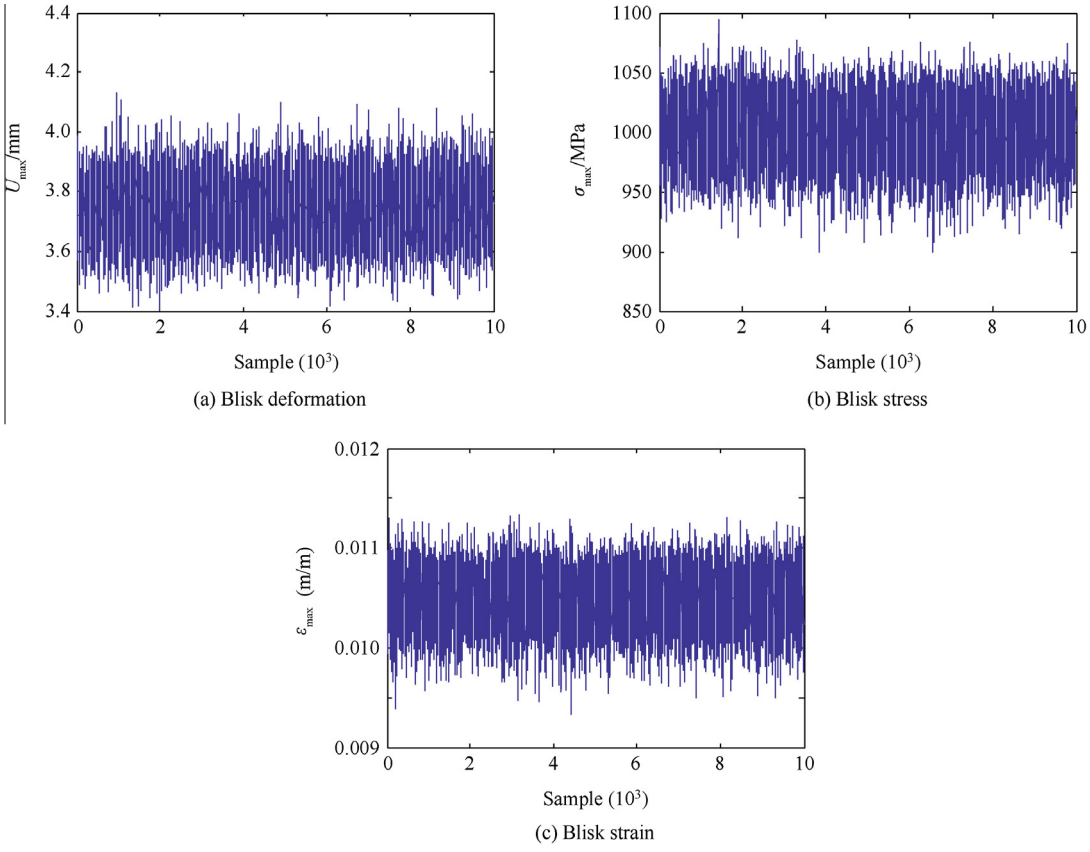

Fig. 10 Simulation histories of blisk deformation, stress and stain.

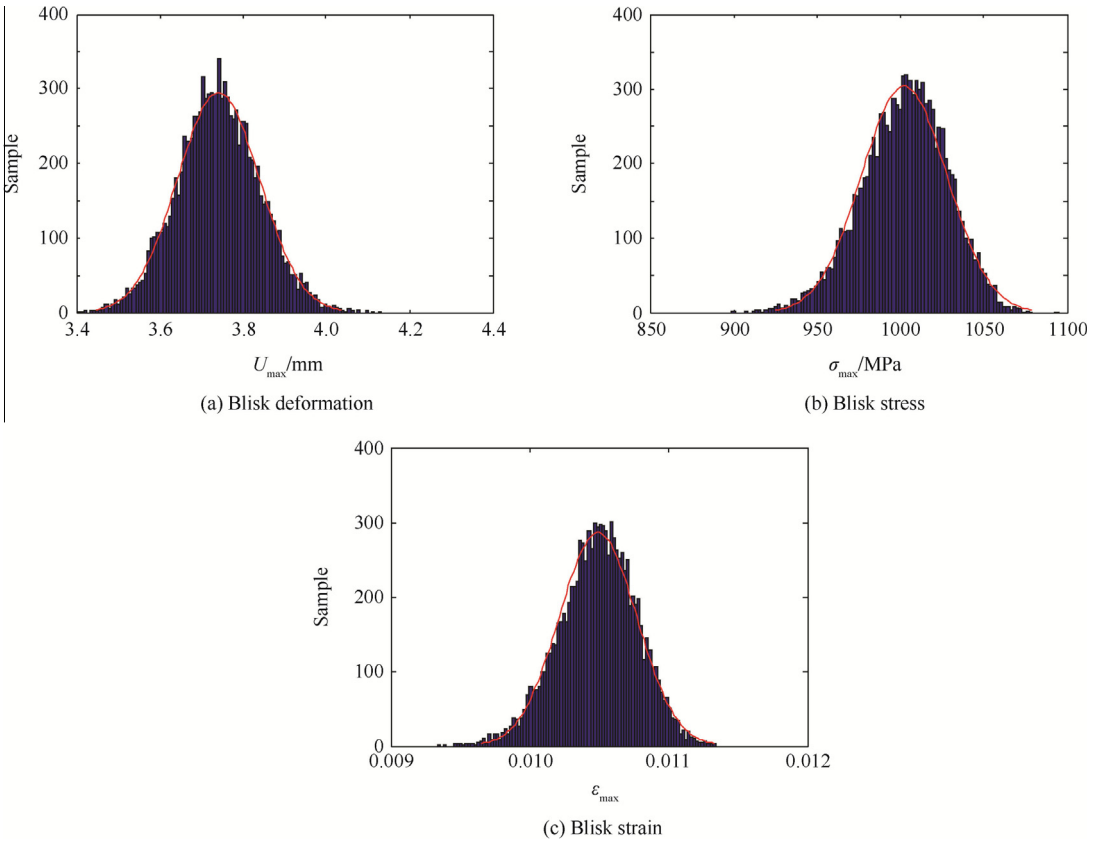

Fig. 11 Distributions of blisk output response.

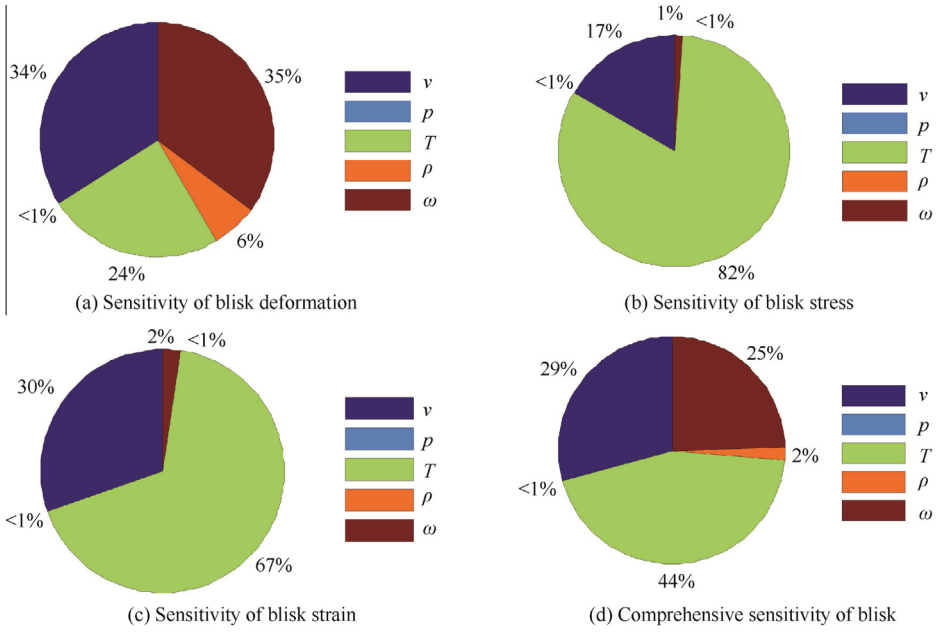

Fig. 12 Results of blisk sensitivity analysis.

4.4. Discussion

As demonstrated from Table 2, Figs. 10 and 11, the reliability degrees of blisk deformation, stress and strain are 99.45%, 99.44% and 99.72% respectively when the designed deformation, stress and strain of blisk are 3.7 m, 1.0023×10^9 Pa and 1.05×10^{-2} m/m. Under this condition, the comprehensive reliability degree of turbine blisk is 0.9931. The results

Table 3 Sensitivities and impact probabilities of input random variables.

Variable	L_1	P_1 (%)	L_2	P_2 (%)	L_3	P_3 (%)	L	P (%)
v	-4.7×10^{-4}	34	-2.0×10^{-4}	17	-7.0×10^{-4}	30	-2.3×10^{-5}	29
p	-1.1×10^{-7}	< 1	-1.8×10^{-9}	< 1	2.1×10^{-7}	< 1	-1.0×10^{-8}	< 1
T	3.3×10^{-4}	24	1.0×10^{-3}	82	1.6×10^{-3}	67	3.5×10^{-5}	44
ρ	8.7×10^{-5}	6	1.7×10^{-7}	< 1	-9.4×10^{-7}	< 1	1.4×10^{-6}	2
ω	4.8×10^{-4}	35	-1.5×10^{-5}	1	5.6×10^{-5}	2	1.9×10^{-5}	25

Note: L_1, L_2, L_3 and L are the sensitivities of input variables for deformation, stress, strain and overall blisk, respectively; P_1, P_2, P_3 and P demote the influencing probabilities of input variables for deformation, stress, strain and overall blisk, respectively.

Table 4 Computational time of blisk reliability analyses with four methods.

Method	Computational time under different simulation numbers (s)			
	10^2	10^3	10^4	10^5
MC method	6940	59800	863000	
RSM	2.36	6.59	17.68	96.28
MRSM	0.87	1.58	5.49	14.08
AMRSM	0.34	0.45	0.76	2.76

Table 5 Computing precision of blisk reliability analyses with four methods.

Simulation number	Reliability degree				Precision (%)		
	MC method	RSM	MRSM	AMRSM	RSM	MRSM	AMRSM
10^2	0.99000	0.96000	0.98000	0.99000	97.98	98.99	100
10^3	0.99300	0.97900	0.99000	0.99200	98.59	99.69	99.90
10^4	0.99310	0.98480	0.99180	0.99320	99.16	99.87	99.99
10^5		0.99082	0.99213	0.99312			

are promising to satisfy the requirement of engineering design.

As revealed by Fig. 12 and Table 3, the inlet gas velocity, temperature and rotating speed are main factors for the total deformation of blisk with the influence probabilities 34%, 24% and 35%, respectively. The effects of the inlet gas velocity and temperature on the stress of blisk are over 98%, in which the influence of gas temperature holds the greatest effect due to its impacting probability over 82%. The main factors of blisk strain are inlet gas velocity and temperature because of their influence probabilities 30% and 67%, respectively.

As shown from the results of comprehensive sensitivity analysis, the main factors of blisk failure are inlet fluid velocity, temperature and rational speed corresponding to the influence probabilities 29%, 44% and 25%, respectively. In the effect of the variables on the failure probability, the variable is positively related with the output response as the sensitivity is positive value, while negative sensitivity indicates that the output response negatively changes with the random variable. Comprehensively considering blisk failure, we can see that the reduction of fluid velocity and fluid pressure causes the increase of blisk failure probability, while the increases of temperature, density and rotational speed lead to the increases of blisk failure probability, which is basically consistent with practical engineering.

As revealed in Table 4 and 5, the computing time of RSM, MRSM and AMRSM is far less than that of MC method. With the increase of the simulation times, the computational efficiency of AMRSM is higher than RSM and MRSM. Thus, the presented AMRSM is proved to hold the highest computational efficiency and speed due to the smallest time consumption. In the aspect of calculation accuracy, AMRSM is almost consistent with MC method, and higher than MRSM and RSM. Therefore, the AMRSM is demonstrated to be a highly accurate and highly efficient approach for reliability analysis.

5. Conclusions

(1) The reliability probability of blisk deformation, stress and strain are 0.9945, 0.9944, 0.9972 and 0.9931, respectively, and the comprehensive reliability degree of turbine blisk is 0.9931 when the designed deformation, stress and strain of turbine blisk are 3.7×10^{-3} m, 1.0023×10^9 Pa and 1.05×10^{-2} m/m.

(2) The inlet gas velocity, temperature and rotating speed are main factors for the total deformation of blisk. The effect probabilities of the inlet gas velocity and tem-

perature on the stress of blisk are about 17% and 82%. The main factors leading to blisk strain are inlet gas velocity and temperature.

(3) As shown from the results of comprehensive sensitivity analysis, the main factors of blisk failure are inlet fluid velocity, temperature and rational speed. Meanwhile, blisk failure is negatively influenced by gas velocity and pressure and positively affected by gas temperature, material density and rotational speed.

(4) AMRSM holds high computational precision and efficiency from the comparison of methods. With the increase of simulation number, the advantages of AMRSM are more obvious. The results demonstrate that AMRSM is a feasible and efficient method for reliability analysis of multiple failure mode structures.

Acknowledgements

This study was co-supported by the National Natural Science Foundation of China (No. 51275138), the Science Foundation of Heilongjiang Provincial Department of Education (No. 12531109), the funding of Hong Kong Scholars Programs (Nos. XJ2015002 and G-YZ90) and China's Postdoctoral Science Funding (No. 2015M580037).

References

1. Sun C, He ZJ, Zhang ZS, Chen XF, Cao HR, Ning XY, et al. Operating reliability assessment for aero-engine based on condition monitoring information. *J Mech Eng* 2013;**49**(6):30–7 [Chinese].
2. Chen YS, Zhang HB. Review and prospect on the research of dynamics of complete aero-engine system. *Acta Aeronaut Astronaut Sin* 2011;**32**(8):1371–9 [Chinese].
3. Gokhale SS, Lyu MR. A simulation approach to structure based software reliability analysis. *IEEE Trans Software Eng* 2005;**31**(8):643–56.
4. Kaymaz I. Application of Kriging method to structural reliability problems. *Struct Saf* 2005;**27**(2):133–51.
5. Lin KK, Shea-Brown E, Young LS. Reliability of coupled oscillators. *J Nonlinear Sci* 2009;**19**(5):497–545.
6. Dimitrov N, Friis-Hansen P, Berggreen C. Reliability analysis of a composite wind turbine blade section using the model correction factor method: Numerical study and validation. *Appl Compos Mater* 2013;**20**(1):17–39.
7. Hu Z, Li HF, Du XP, Chandrshekhara K. Simulation-based time-dependent reliability analysis for composite hydrokinetic turbine blades. *Struct Multidiscip Optim* 2013;**47**(5):765–81.
8. Wang L, Wang X, Xia Y. Hybrid reliability analysis of structures with multi-source uncertainties. *Acta Mech* 2014;**225**(2):413–30.
9. Zhang CY, Bai GC. Extremum response surface method of reliability analysis on two-link flexible robot manipulator. *J Cent South Univ* 2012;**19**(1):101–7.
10. Krishnamurthy T. Comparison of response surface construction methods for derivative estimation using moving least squares, Kriging and radical basis functions. *Proceedings of 46th AIAA/ASME/ASCE/AHS/ASC structures, structural dynamics, and materials conference*; 2005 April 18–20; Austin 485 (TX). Reston: AIAA; 2005. p. 182–7.
11. Xiong FF, Liu Y, Xiong Y, Yang SX. A double weighted stochastic response surface method for reliability analysis. *J Mech Sci Technol* 2012;**26**(8):2573–80.
12. Fei CW, Bai GC. Nonlinear dynamic probabilistic analysis for turbine casing radical deformation using extremum response surface method based on support vector machine. *J Comput Nonlinear Dyn* 2013;**8**(4):041004.
13. Fei CW, Bai GC. Dynamic probabilistic design for blade deformation with SVM-ERSM. *Aircr Eng Aerosp Technol* 2015;**87**(4):1–14.
14. Ren Y, Bai GC. New neural network response surface methods for reliability analysis. *Chin J Aeronaut* 2011;**24**(1):25–31.
15. Lv ZZ, Yang ZZ, Zhao J. An artificial neural network method for reliability analysis based on weighted linear response surface. *Chin J Aeronaut* 2006;**27**(6):1063–7.
16. Bai B, Bai GC. Dynamic probabilistic analysis of stress and deformation for bladed disk assemblies of aeroengine. *J Cent South Univ* 2014;**21**(10):3722–35.
17. Fei CW, Bai GC. Distributed collaborative extremum response surface method for mechanical dynamic assembly reliability analysis. *J Cent South Univ* 2013;**20**(9):2414–22.
18. Bai GC, Fei CW. Distributed collaborative response surface method for mechanical dynamic assembly reliability design. *Chin J Mech Eng* 2013;**38**(4):1160–8.
19. Zhai X, Fei CW, Zhai QG, Wang JJ. Reliability and sensitivity analyses of HPT blade-tip radical running clearance using multiply response surface model. *J Cent South Univ* 2014;**21**(11):4368–77.
20. Malhotra R, Negi A. Reliability modeling using particle swarm optimization. *Int J Syst Assur Eng Manage* 2013;**4**(3):275–83.
21. Liu DX, Cao CX. *Handbook of materials for aircraft engine design*. 4th ed. Beijing: Aviation Industry Press; 2010. p. 403–17 [Chinese].
22. Hua C, Fang C. Simulation of fluid–solid interaction on water ditching of an airplane by ALE method. *J Hydrodyn* 2011;**23**(5):637–42.

Zhang Chunyi is a professor at School of Mechanical and Power Engineering, Harbin University of Science and Technology, Harbin, China. He received his Ph.D. degree in aerospace engineering from Beihang University in 2011. His research interests are mechanical structural strength, reliability design and optimization.

Song Lukai is a Ph.D. student at School of Energy and Power Engineering, Beihang University. He received his M.S. degree in mechanical engineering from Harbin University of Science and Technology in 2016. His research interests are aeroengine structural reliability design and optimization.

Fei Chengwei is a research fellow at Department of Mechanical Engineering, The Hong Kong Polytechnic University, Kowloon, Hong Kong, China. He received his Ph.D. degree in aerospace engineering from Beihang University in 2014. His research interests are aeroengine structural strength, vibration and reliability.

Lu Cheng is a Ph.D. student at School of Aeronautics, Northwestern Polytechnical University. He received his M.S. degree in mechanical engineering from Harbin University of Science and Technology in 2016. His research interests are aircraft structural reliability design and optimization.

Xie Yongmei is an M.S. student at School of Mechanical and Power Engineering, Harbin University of Science and Technology, Harbin, China. His research interests are mechanical reliability design and optimization.